

Published in final edited form as:

*Biol Psychiatry*. 2013 September 15; 74(6): 467–474. doi:10.1016/j.biopsych.2013.02.029.

## Disruption of Anterior Insula Modulation of Large-Scale Brain Networks in Schizophrenia

Lauren V. Moran, MD<sup>1,\*</sup>, Malle A. Tagamets, PhD<sup>1</sup>, Hemalatha Sampath, MS<sup>1</sup>, Alan O'Donnell<sup>1</sup>, Elliot A. Stein, PhD<sup>2</sup>, Peter Kochunov, PhD<sup>1</sup>, and L. Elliot Hong, MD<sup>1</sup>

<sup>1</sup>Maryland Psychiatric Research Center, Department of Psychiatry, University of Maryland School of Medicine, Baltimore, Maryland 21228 <sup>2</sup>Neuroimaging Research Branch, National Institute on Drug Abuse-Intramural Research Program, National Institutes of Health, Baltimore, Maryland

### Abstract

**Background**—Systems level modeling of fMRI data has demonstrated dysfunction of several large-scale brain networks in schizophrenia. Anomalies across multiple functional networks associated with schizophrenia could be due to diffuse pathology across multiple networks or alternatively, dysfunction at a converging control(s) common to these networks. The right anterior insula has been shown to modulate activity in the central executive and default mode networks in healthy individuals. We tested the hypothesis that right anterior insula modulation of central executive and default mode networks is disrupted in schizophrenia and is associated with cognitive deficits.

**Methods**—In 44 patients with schizophrenia and 44 healthy controls, we used seed-based resting state functional connectivity fMRI analysis to examine connectivity between right insular subregions and central executive/default mode network regions. We also performed two directed connectivity analyses of resting state data: Granger analysis and confirmatory structural equation modeling. Between-group differences in path coefficients were used to evaluate anterior insula modulation of central executive and default mode networks. Cognitive performance was assessed using the rapid visual information processing task, a test of sustained attention.

**Results**—Using multiple connectivity techniques, we found compelling, corroborative evidence of disruption of right anterior insula modulation of central executive and default mode networks in patients with schizophrenia. The strength of right anterior insula modulation of these networks predicted cognitive performance.

**Conclusions**—Individuals with schizophrenia have impaired right anterior insula modulation of large-scale brain networks. The right anterior insula may be an emergent pathophysiological gateway in schizophrenia.

© 2013 Society of Biological Psychiatry. Published by Elsevier Inc. All rights reserved.

\*Correspondence to, Maryland Psychiatric Research Center, P.O. Box 21247, Baltimore, MD 21228. Tel: 410 402 6827. Fax: 410 402 6023. l Moran@mprc.umaryland.edu. .

**Financial Disclosures:** The authors report no biomedical financial interests or potential conflicts of interest.

**Publisher's Disclaimer:** This is a PDF file of an unedited manuscript that has been accepted for publication. As a service to our customers we are providing this early version of the manuscript. The manuscript will undergo copyediting, typesetting, and review of the resulting proof before it is published in its final citable form. Please note that during the production process errors may be discovered which could affect the content, and all legal disclaimers that apply to the journal pertain.

## Keywords

schizophrenia; imaging; anterior insula; salience network; default mode network; central executive network

---

## Introduction

Pathophysiological observations in schizophrenia range from numerous genes, regional anatomical and functional brain abnormalities to global, system-level brain dysfunction (1, 2). Large-scale brain network analysis of fMRI data acquired in the resting state has been increasingly employed in studies of schizophrenia and other psychiatric disorders (3, 4). Resting state functional connectivity (rsFC) measures the low frequency coherence in the blood oxygenation level dependent (BOLD) signal during the task-free resting state, leading to the identification of a set of ‘core’ networks with highly coherent activity (5, 6).

Three large-scale networks have garnered much of the attention: the central executive (CEN), salience (SN), and default mode networks (DMN) (4). Task-positive regions consistently activated across cognitive tasks have been dissected into two distinct networks: CEN and SN. The CEN, comprised of dorsolateral prefrontal cortex (DLPFC), inferior parietal lobule/sulcus (IPL) and associated subcortical regions (e.g., dorsal caudate) (7, 8), is associated with focused attention on the external environment during demanding cognitive tasks. The SN, composed of the anterior insula (AIns) and dorsal anterior cingulate (dACC) (7), mediates selection of physiologically relevant external and interoceptive signals. In contrast, the DMN is a set of regions consistently deactivated during cognitive tasks and is anticorrelated with the CEN (9). The DMN, composed of posterior cingulate cortex (PCC), medial prefrontal cortex (MPFC), lateral parietal cortex and parahippocampal gyrus, is conceptualized as multiple dissociated networks subserving self-referential internally directed thought (10). The strength of anticorrelation between CEN and DMN is associated with more consistent performance on demanding tasks (11).

In schizophrenia, isolated abnormalities in all three networks have been linked to cognitive impairments (12-15). In addition, deficient upregulation of task-positive networks coupled with reduced suppression of DMN is a replicated finding in schizophrenia, indicating faulty interaction of these networks (13, 16). Decreased efficiency of task-positive networks and DMN is associated with impaired working memory capacity in schizophrenia (17). A critical question is whether these perturbations in network interactions are secondary to diffuse dysfunction in multiple networks or are due to centralized malfunction at a controlling hub common to these regions.

In contrast to standard rsFC approaches that measure temporal correlation between activity across different brain regions, directional connectivity techniques (18, 19) investigate the directed influence of a node on network dynamics. Converging evidence in healthy individuals using various directed connectivity techniques suggests that the *right* AIns, a key node of the SN, is a major outflow hub that selectively influences activity in both CEN and DMN and has been proposed to switch between these two networks (8, 20, 21). AIns modulation of large-scale networks is lateralized and specific to the right AIns, possibly related to its role in interoceptive awareness of physically and emotionally arousing stimuli such as pain (22, 23), or to right-hemisphere lateralization of sympathetic nervous system control (24).

The AIns is critically involved in task initiation, maintenance of attention and performance monitoring (25, 26), all found to be impaired in schizophrenia (27, 28). Furthermore, AIns

findings in schizophrenia (29) include reduced volume in first episode and chronic schizophrenia (30) and abnormal right AIns activation across a variety of executive function tasks (31). Thus, it is feasible that abnormal CEN/DMN interactions observed in schizophrenia (13, 16, 17) are mediated through a faulty right AIns hub. We therefore hypothesize that right AIns modulation of CEN and DMN is impaired in schizophrenia. We predict that 1) using rsFC, schizophrenia subjects will have decreased rsFC between the right AIns and major hubs of the CEN and DMN; 2) using two independent directed connectivity techniques, Granger analysis and confirmatory structural equation modeling (SEM), subjects with schizophrenia will have significantly abnormal outflow from right AIns to CEN/DMN regions; and 3) right AIns modulation of CEN and DMN will correlate with performance on a sustained attention task.

## Methods and Materials

### Subjects

Fifty patients with schizophrenia recruited from outpatient clinics and 50 normal controls recruited from the local community signed informed consent approved by local IRBs prior to any study procedures. Diagnosis of schizophrenia was confirmed by the Structured Clinical Interview for DSM-IV (32). All patients were clinically stable on antipsychotic medications (mean  $\pm$  SD chlorpromazine equivalent dose  $411 \pm 417$  mg) (33). Three patients were also on mood stabilizers and two were on antidepressants. Controls did not have any Axis I psychiatric diagnoses or first-degree relatives with psychotic illness.

Data on 44 controls and 44 schizophrenia patients were included in final analyses due to head motion in 12 subjects (see Supplement for details). The groups did not differ with respect to age (mean  $\pm$  SD: controls  $37.9 \pm 11.0$ , schizophrenia  $35.2 \pm 12.1$ ;  $t=1.1$ ,  $p=0.28$ ) and gender (F:M: controls 7:37, schizophrenia 4:40,  $\chi^2=0.9$ ,  $p=0.33$ ).

### Clinical and Cognitive Parameters

Severity of symptoms in patients was measured using the Brief Psychiatric Rating Scale (BPRS) (34) total, positive and negative symptom scores. A subset of subjects (23/44 controls; 40/44 schizophrenia) underwent testing with the rapid visual information processing (RVIP) task, a continuous performance task of sustained attention, performed in the scanner during the same session that resting state data were acquired. Single digits were successively presented for 600 msec. The subject pressed a button whenever three odd or three even numbers in a row appeared (35). Performance was measured using d-prime, an overall measure accounting for both target detection and false alarm rates. Two-tailed t-tests compared d-prime in patients and controls.

### MRI Data Acquisition

Subjects were scanned on a 3-T MR Siemens Allegra scanner (quadrature volume head coil) and were instructed to rest with eyes open and not think of anything in particular for five minutes. High resolution ( $1 \times 1 \times 1$  mm<sup>3</sup>) T1-weighted MPRAGE images were acquired. Functional MR images were acquired over 39 axial, interleaving, 4-mm sections by means of a gradientecho echoplanar imaging sequence (150 volumes; echo time/repetition time 27/2000 milliseconds; flip angle 80°; field of view  $220 \times 220$  mm<sup>2</sup>; image matrix  $64 \times 64$ ). Resting state data was acquired first to avoid task-related carryover effects.

### Statistical Analysis

**Cluster Analysis**—Because previous studies indicate that the insula is functionally divided into three subregions [dorsal anterior (dAIns), ventral anterior (vAIns) and posterior

(PIIns insula (26, 36-38)], we functionally parcellated the insula into three regions. The right insula was first identified by manual drawing on the T127 MNI template and resampled to  $3 \times 3 \times 3 \text{ mm}^3$  space. Each insular voxel was used as a seed region for functional connectivity analyses. Cluster analysis was performed using data-driven k-means clustering analysis on insular voxel functional connectivity profiles similar to Deen et al (36). See Supplement for details of clustering analysis/preprocessing.

**Functional Connectivity**—Using the three insular clusters as seed regions, z-transformed correlation coefficients [ $z(r)$ ] were calculated between the average time course in each seed and the whole brain (voxelwise). Functional connectivity analyses were performed 1) to look for areas with statistically significant differences in functional connectivity with insula seeds between control and schizophrenia subjects (two-tailed independent samples t-test) and 2) to select nodes for Granger analysis, using areas with significant connectivity with AIns seeds.

To further test the specificity of insula-centric modulation of CEN and DMN in schizophrenia, we performed two “reversed” whole-brain functional connectivity analyses using key hubs of the CEN (DLPFC) and DMN (PCC) as seed regions. See Supplement for details.

**Directed Functional Connectivity Modeling – Network Node Selection**—Node selection methods resulted in thirteen regions that represented the three networks of interest (Figure S1, Table 1): **CEN**: DLPFC, IPL and caudate (7); **SN**: 3 insular subregions identified by cluster analysis and 3 anterior cingulate areas: dACC, pregenual anterior cingulate (pgACC) and the posterior part of dACC and middle cingulate cortex (midACC) (7); and **DMN**: PCC, MPFC, lateral parietal, and parahippocampal regions (5, 39). See Supplement for node selection methods.

**Directed Functional Connectivity: Granger Analysis**—We used a vector autoregression (Granger) approach to examine time lagged effects between brain regions to determine directionality of influence. Granger analysis was performed for each subject using the AFNI program 1dGC.R (40) using time series extracted from each of the 13 nodes. Path coefficients from Granger analysis indicate the strength and direction of the relationship between two regions within a network, similar to regression coefficients with the addition of directional information. Each subject’s path coefficients and associated t-statistics were entered into a multivariate linear mixed-effects analysis for group analysis. See Supplement for details.

To allow for correlations with individual subject clinical and cognitive parameters, we calculated the mean path coefficient for each node to areas of the CEN, SN and DMN for each subject. For example, to calculate right dAIns→CEN, we averaged path coefficients from right dAIns→IPL, dAIns→DLPFC, and dAIns→caudate for each subject. Within-network connectivity measures were calculated as mean path coefficients from a node to other areas within the same network (e.g., dAIns→SN reflects outflow from dAIns to other functional subdivisions of insula and ACC regions). After finding significant group differences in these node-to-network mean path coefficients (two-tailed t-tests), we calculated Pearson’s correlation coefficients between these measures and d-prime (from RVIP task) and symptom severity scores (BPRS total, positive and negative symptom subscales) to determine if cognitive performance and/or symptom severity are related to each node-to-network modulation. Correlations between node-to-network measures and d-prime were performed across all subjects. Fisher r-to-z transformation was used to calculate z-values to assess if correlation coefficients significantly differed between groups. In the

event of a significant difference in correlation coefficients between groups, correlations were also performed for each group separately, corrected for multiple comparisons.

**Effective Connectivity: Structural Equation Modeling (SEM)**—In contrast to data-driven Granger analysis, SEM is a confirmatory effective connectivity technique that examines instantaneous relationships between network regions. SEM requires input of a hypothesized model of interactions. A simplified network of 4 ROIs was selected that included right dAIns and a representative region of the three major networks: CEN (DLPFC), SN (dACC) and DMN (MPFC). The input model for controls included dAIns→CEN, dAIns→dACC and dAIns→MPFC. Based on Granger analysis results, we also included dACC→dAIns and reciprocal connections between DLPFC and MPFC. Separate models were fit to schizophrenia and control data. To assess model fit model, we used a combination of  $\chi^2$  goodness of fit, root-mean-square error of approximation (RMSEA) and adjusted goodness of fit index (GFI). Stacked models were used for group comparisons (see Supplement for details).

## Results

### Cluster Analysis

Cluster analysis segregated the right insula into dAIns, vAIns, and PIns for both groups (Figure 1, Table S1). See Supplement for details.

### Functional Connectivity Analysis

Using insula clusters as seed regions, rsFC analysis revealed distinct patterns of connectivity for the three subregions consistent with previous reports (26, 36-38). All three insular regions had strong functional connections with the anterior cingulate, another key node of the SN, in anatomically parallel anterior-posterior procession: vAIns connected to pgACC, dAIns connected to dACC and PIns connected to midACC. The dAIns was strongly connected with areas of the CEN: DLPFC, IPL and dorsal caudate. In contrast, the vAIns had strong connectivity with limbic areas, such as parahippocampal gyrus. The PIns exhibited connectivity with frontal and subcortical (thalamus and midbrain) areas. These distinct patterns of connectivity were consistent between control and schizophrenia subjects (Figure S2).

Two-tailed t-tests revealed significant group differences in right vAIns rsFC (Table 2, Figure 2A-C). Of note, clusters involved key nodes of the DMN: MPFC, PCC and bilateral lateral parietal cortex (5). While rsFC between the right vAIns and DMN regions was positively correlated in controls, there was a lack of significant connectivity in schizophrenia (Figure 2D).

For whole brain rsFC analyses using key hubs of the CEN (DLPFC) and DMN (PCC) as seeds (5, 13), only one region showed significantly decreased connectivity in schizophrenia for both CEN and DMN seeds: an overlapping cluster spanning the posterior portion of right AIns and anterior portion of PIns (right anterior-mid insula) (Figure 3; Table 2). Thus, consistent with our hypothesis, patients with schizophrenia exhibited decreased connectivity exclusively between the right insula and key hubs of CEN and DMN.

There were no significant correlations between chlorpromazine equivalent dose and connectivity between right vAIns and DMN regions or connectivity between CEN/DMN hubs and the right insula (all  $p > 0.35$ ), suggesting findings were not due to antipsychotic medication.

### Directed Functional Connectivity Modeling – ROI Selection

In addition to the 3 insular divisions identified from cluster analysis, selecting right hemisphere regions with strong connectivity to AIns seeds resulted in an additional 7 nodes (3 anterior cingulate regions, DLPFC, IPL, caudate, parahippocampal cortex; Table S2). Areas within the DMN that showed significant group differences in the right vAIns seed-based rsFC analyses resulted in an additional 3 nodes (MPFC, PCC and right lateral parietal cortex). These 13 nodes (Figure S1) were central to our hypothesis of faulty AIns modulation of CEN and DMN. Table 1 lists node coordinates.

### Directed Functional Connectivity – Granger Analysis

Results in controls showed that the right AIns is a hub with positive outflow to areas of all three networks (8, 20) (Figure 4A). In contrast, subjects with schizophrenia had diminished dAIns-to-CEN and dAIns-to-DMN network interactions (Figure 4B). Group comparison revealed significant decreases in path coefficients in schizophrenia for dAIns→DLPFC, dAIns→PCC, dAIns→lateral parietal and caudate→DLPFC (false discovery rate  $p_{corrected} < 0.05$ ; Figure 4C). The strongest paths for controls and the most significantly decreased paths in schizophrenia by group comparison were outflow from the right dAIns. Additional secondary analyses in Supplement support these findings.

For individual subject node-to-network measures, there was a significant decrease in dAIns→CEN ( $t=2.1$ ,  $p=0.04$ ), dAIns→other areas of SN ( $t=2.2$ ,  $p=0.03$ ) and dAIns→DMN ( $t=4.1$ ,  $p<0.001$ ) for the schizophrenia group compared with controls (Figure S3A). There were no significant differences for the other 12 ROIs. The dAIns→DMN was statistically significant after correcting for multiple comparisons [ $0.05/(13 \times 3)=0.001$ ]. In patients, there were no significant correlations between any node-to-network measure and chlorpromazine equivalent dose (all  $p>0.1$ ) or BPRS scores (all  $p>0.05$ ).

### RVIP performance and strength of AIns modulation of CEN/DMN

For the RVIP task, patients with schizophrenia had significantly poorer performance than controls (d-prime: mean  $\pm$  SD:  $4.4 \pm 1.5$  controls vs.  $2.5 \pm 2.0$  schizophrenia,  $t=4.1$ ,  $p<0.001$ ). After correcting for the maximum number of correlations performed [ $p=0.05/(3 \text{ dAIns node-to-network measures} \times 3 \text{ groups})=0.004$ ], we found significant correlations between dAIns→DMN and d-prime in the combined sample ( $r=0.46$ ,  $p<0.001$ ; Figure S3B) without significant difference in correlation coefficients in controls vs. schizophrenia analyzed separately ( $z=1.0$ ,  $p=0.33$ ). Since correlations across the whole group could be driven by group differences, we performed a post-hoc regression analysis between d-prime (dependent variable) and dAIns→DMN (independent variable) including group status as a factor to control for diagnosis and still found a significant relationship between d-prime and dAIns→DMN, albeit less significant [ $F(2,60)=10.3$ ,  $p<0.001$ ; dAIns→DMN  $t=2.4$ ,  $p=0.02$ ]. There was no significant interaction between diagnosis and dAIns→DMN.

We found a nominally significant positive correlation between dAIns→CEN and d-prime in the combined sample ( $r=0.32$ ,  $p=0.01$ ). The correlation coefficients between the two groups significantly differed ( $z=3.1$ ,  $p=0.002$ ), with a significant correlation between dAIns→CEN and d-prime for controls ( $r=0.71$ ,  $p<0.001$ ; significant after correction) but not in schizophrenia ( $r=0.03$ ,  $p=0.86$ ).

### Effective Connectivity – Structural Equation Modeling

Consistent with Granger analysis, SEM analysis revealed positive path coefficients from dAIns→DLPFC, dAIns→dACC, and dAIns→MPFC in controls (Figure S4A), with  $\chi^2$  goodness of fit = 2.21,  $p=0.53$ ; RMSEA $<0.05$ , and GFI=0.92, indicating good fit of model. The strongest paths were positive influence of dAIns→DLPFC and negative influence of



DLPFC→MPFC. Group comparison of individual paths indicated significantly decreased dAIns→DLPFC, dAIns→MPFC, MPFC→DLPFC, and less negative DLPFC→MPFC path coefficients for schizophrenia subjects (all  $p_{\text{corrected}} < 0.001$ , Bonferroni corrected for number of paths in model). Thus, SEM analysis demonstrated diminished positive outflow from dAIns to CEN and DMN in schizophrenia.

As a supportive analysis, we repeated the analysis for schizophrenia data. Note the absence of paths from dAIns to both CEN (DLPFC) and DMN (MPFC) for the model that fit schizophrenia data (Figure S4B). Significant group differences in path coefficients for remaining paths were consistent with those identified using the control model (MPFC→DLPFC, DLPFC→MPFC; all  $p_{\text{corrected}} < 0.001$ ). Fit parameters indicated good fit of model to data:  $\chi^2 = 2.39$ ,  $p = 0.50$ ; RMSEA  $< 0.05$ ; GFI = 0.91.

In summary, SEM analyses using models that fit control or conversely schizophrenia group data consistently identified significant decreases in path strength of dAIns→CEN and dAIns→DMN in schizophrenia.

## Discussion

The key novel finding of this study is disruption of right AIns functional connectivity with default mode and central executive networks in schizophrenia using reciprocated node-to-node analyses. By applying methodologically distinct *directed* functional connectivity network analyses, i.e., Granger analysis and structural equation modeling, we demonstrated that the multiple network dysfunctions observed in schizophrenia may originate from impaired right AIns modulation.

Our most robust finding is the convergence of results from bivariate functional connectivity (using either insular clusters or CEN/DMN hubs as seeds), Granger analysis and SEM in demonstrating dysfunctional AIns modulation of CEN/DMN in schizophrenia. Because of controversy over the interpretation of Granger analysis (41-44), we employed SEM as a confirmatory technique. Granger analyses were nonetheless critical since individual subject analyses were performed prior to group analysis. Individual subject analyses allowed the study a more extensive network compared to SEM (degrees of freedom for individual Granger analyses determined by number of time points in fMRI timeseries) and to use subject path coefficients for correlational analysis. Using Granger analysis, we demonstrated that right AIns outflow to CEN and DMN correlated with performance on a sustained attention task.

### AIns: a network control center

Consistent with previous work (8, 20, 21), we found that the right AIns is a major hub with directed influence over CEN and DMN in healthy individuals. The functional centrality of the AIns may be linked to its known role in affective and cognitive integration (36, 37). The AIns, a key hub of the SN, mediates interoceptive awareness of physiological activity in response to salient stimuli leading to mobilization of brain networks in preparation for shifts of attention or motor responses (45). A parsimonious model of network interactions is that the AIns alternately directs activity between CEN and DMN in response to environmental or physiological demands. This “switching” mechanism (8) is consistent with our finding of *positive* correlations between the AIns and CEN and DMN in the functional connectivity analyses in controls, as these networks are anticorrelated (5) and are dynamically activated (CEN) and deactivated (DMN) during cognitive tasks (46). We also found positive correlations between cognitive performance and both dAIns→CEN and dAIns→DMN measures in controls. One interpretation is that the capacity of the AIns to effectively switch between networks is associated with improved performance. Our corroborative networks

analysis strategy showed that in controls, CEN hubs negatively influence DMN hubs (Granger: DLPFC→MPFC and IPL→PCC; SEM: DLPFC→MPFC). Therefore, although the AIns does not directly deactivate DMN, CEN hubs downregulated DMN activity in both directed connectivity analyses (Figures 4A and S4A). Thus, AIns activation of CEN during cognitive tasks may indirectly lead to DMN downregulation, a dynamic process that may be impaired in schizophrenia.

### Network abnormalities in schizophrenia

Previous literature has described disruption of large-scale networks in schizophrenia. Although there are some reports of increased connectivity such as hyperconnectivity within the DMN (13), systematic reviews of the literature point to hypoconnectivity, with decreased connectivity between the PFC and various cortical/subcortical nodes being the most common finding (47, 48). Other reports of dysfunction in CEN, SN and DMN in schizophrenia include a lack of connectivity between MPFC and insula (49), decreased ability to upregulate task-positive regions (16, 50), and reduced anticorrelation between CEN and DMN (13). Our finding of decreased right AIns modulation of CEN and DMN in schizophrenia provide an overarching framework by proposing that some of the diffuse abnormalities observed in these networks in previous studies (13, 16, 17) may at least in part originate from a deficient right AIns control mechanism. For example, decreased AIns modulation between CEN is consistent with decreased recruitment of or hypoconnectivity between frontal and other CEN nodes (47, 50). Hyperconnectivity within the DMN could be mediated by faulty AIns activation of CEN-mediated downregulation of DMN.

### AIns modulation of CEN and DMN: cognitive deficits

Cognitive deficits are a core feature of schizophrenia (51). CEN and DMN impairments have been linked to performance deficits in cognitive tasks in patients with schizophrenia (13, 16). Localized dysfunctions such as hypo- or hyperactivation of the DLPFC and other CEN nodes are consistently associated with cognitive impairments in schizophrenia (31, 50, 52). Importantly, we found directed path coefficients from right dAIns→CEN and dAIns→DMN that significantly correlated with RVIP performance, a task requiring sustained attention and working memory (53). Our data offer a systems-level, alternative framework suggesting that the ability of the AIns to modulate CEN and DMN contributes to deficits in sustained attention, one of the most robust and consistently observable cognitive deficits in schizophrenia (28, 54). Other studies have implicated right AIns pathology in frontotemporal dementia (55, 56) and autism (57, 58). In addition, loss of integrity of white matter tracts involving AIns has been associated with abnormal DMN function in traumatic brain injury (59). Together, these studies suggest that disrupted AIns modulation of CEN and DMN may contribute to cognitive impairments across a variety of neuropsychiatric disorders in addition to schizophrenia (4).

Although a strong correlation between dAIns→CEN and d-prime was found in controls, there was no significant correlation in schizophrenia. One explanation is that, because of disrupted dAIns→CEN outflow, other compensatory regions were recruited to activate CEN that better explain the variance in cognitive performance. For example, schizophrenia subjects had significantly greater positive outflow from caudate→DLPFC in the Granger analysis, suggesting that subcortical compensatory routes may be recruited.

### Limitations

Interpretation of our data must be taken in view of several limitations. All subjects were on antipsychotic medications. However, there were no significant correlations between antipsychotic medication dose and dAIns-to-CEN/SN/DMN or any other node-to-network



path coefficients for the Granger analysis, and no significant correlations between dose and functional connectivity between AIns and CEN/DMN regions.

Granger analysis of fMRI data is an exploratory method limited by potentially spurious directionality due to variability in the hemodynamic response function (41, 60). Critics argue that lagged effects in the BOLD signal are too slow for realistic modeling of neural communication between regions (41). Therefore, Granger analysis results should be interpreted with caution. However, since rsFC is a measure of low frequency synchronizations in the BOLD signal (< 0.1 Hz), lagged effects of slow oscillatory activity in this frequency range could potentially be modeled. The neural correlates of low frequency BOLD synchronizations are unclear but some evidence suggests they may reflect underlying low frequency neuronal oscillatory activity that may modulate higher frequency neuronal activities. For example, low frequency fluctuations (<0.1 Hz) in high-gamma-band (65-110 Hz) electrical signal coherence between DMN regions has been identified (61), corresponding to the frequency of rsFC BOLD signals used to estimate our Granger analysis models. SEM, a method based on instantaneous correlations, provided support for the results of the Granger analyses by confirming the finding of disrupted right AIns outflow to CEN/DMN in schizophrenia. Furthermore, right AIns modulation of outflow to CEN/DMN found in healthy controls is consistent with other studies using either Granger (8) or partial correlation analysis (20), which has been suggested by critics of Granger analysis to be a robust method (41).

Our findings are limited to the nodes and models selected for analysis. We cannot exclude the possibility that including additional nodes may have altered the findings for directional analyses, or that other models may have also provided a good fit using SEM. We acknowledge that both the functional and effective connectivity analyses assume temporal stationarity, prohibiting the study of true dynamic changes in network interaction. Future studies using task-based studies coupled with methods able to measure dynamic changes in network activity are required to confirm dysfunctional AIns 'switching' between CEN and DMN in schizophrenia. We finally note that Granger, SEM and other commonly used techniques to examine the interaction of regions using fMRI data cannot prove causality.

## Conclusion

We showed a centrifugal positive influence of the right AIns over CEN and DMN nodes in controls during resting state (8). This mechanism is significantly weakened in schizophrenia in association with cognitive deficits. An integrated network analysis as deployed here provides a powerful means to model diverse brain imaging observations and leads to the characterization of a likely emergent common pathway in schizophrenia.

## Supplementary Material

Refer to Web version on PubMed Central for supplementary material.

## Acknowledgments

Financial support was received from National Institutes of Health grants T32MH067533, R01DA027680, R01MH085646 and R21DA033817. This research was also supported by the NIDA Intramural Research Program, NIH.

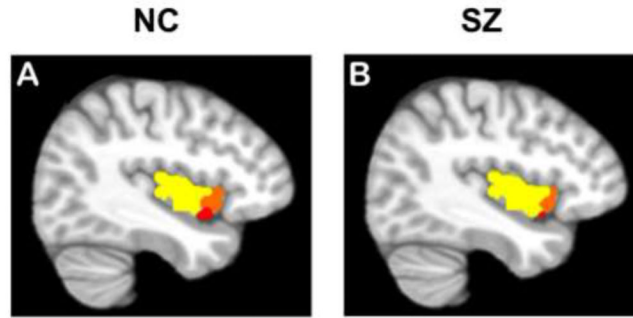
## References

1. Meyer-Lindenberg A, Weinberger DR. Intermediate phenotypes and genetic mechanisms of psychiatric disorders. *Nat Rev Neurosci*. 2006; 7:818–827. [PubMed: 16988657]

2. Lewis DA, Sweet RA. Schizophrenia from a neural circuitry perspective: advancing toward rational pharmacological therapies. *J Clin Invest.* 2009; 119:706–716. [PubMed: 19339762]
3. Lynall ME, Bassett DS, Kerwin R, McKenna PJ, Kitzbichler M, Muller U, et al. Functional connectivity and brain networks in schizophrenia. *J Neurosci.* 2010; 30:9477–9487. [PubMed: 20631176]
4. Menon V. Large-scale brain networks and psychopathology: a unifying triple network model. *Trends in cognitive sciences.* 2011; 15:483–506. [PubMed: 21908230]
5. Fox MD, Snyder AZ, Vincent JL, Corbetta M, Van Essen DC, Raichle ME. The human brain is intrinsically organized into dynamic, anticorrelated functional networks. *Proc Natl Acad Sci U S A.* 2005; 102:9673–9678. [PubMed: 15976020]
6. Greicius MD, Krasnow B, Reiss AL, Menon V. Functional connectivity in the resting brain: a network analysis of the default mode hypothesis. *Proc Natl Acad Sci U S A.* 2003; 100:253–258. [PubMed: 12506194]
7. Seeley WW, Menon V, Schatzberg AF, Keller J, Glover GH, Kenna H, et al. Dissociable intrinsic connectivity networks for salience processing and executive control. *J Neurosci.* 2007; 27:2349–2356. [PubMed: 17329432]
8. Sridharan D, Levitin DJ, Menon V. A critical role for the right fronto-insular cortex in switching between central-executive and default-mode networks. *Proc Natl Acad Sci U S A.* 2008; 105:12569–12574. [PubMed: 18723676]
9. Raichle ME, MacLeod AM, Snyder AZ, Powers WJ, Gusnard DA, Shulman GL. A default mode of brain function. *Proc Natl Acad Sci U S A.* 2001; 98:676–682. [PubMed: 11209064]
10. Buckner RL, Andrews-Hanna JR, Schacter DL. The brain’s default network: anatomy, function, and relevance to disease. *Ann N Y Acad Sci.* 2008; 1124:1–38. [PubMed: 18400922]
11. Kelly AM, Uddin LQ, Biswal BB, Castellanos FX, Milham MP. Competition between functional brain networks mediates behavioral variability. *Neuroimage.* 2008; 39:527–537. [PubMed: 17919929]
12. Garrity AG, Pearlson GD, McKiernan K, Lloyd D, Kiehl KA, Calhoun VD. Aberrant “default mode” functional connectivity in schizophrenia. *Am J Psychiatry.* 2007; 164:450–457. [PubMed: 17329470]
13. Whitfield-Gabrieli S, Thermenos HW, Milanovic S, Tsuang MT, Faraone SV, McCarley RW, et al. Hyperactivity and hyperconnectivity of the default network in schizophrenia and in first-degree relatives of persons with schizophrenia. *Proc Natl Acad Sci U S A.* 2009; 106:1279–1284. [PubMed: 19164577]
14. White TP, Joseph V, Francis ST, Liddle PF. Aberrant salience network (bilateral insula and anterior cingulate cortex) connectivity during information processing in schizophrenia. *Schizophr Res.* 2010; 123:105–115. [PubMed: 20724114]
15. Zhou Y, Liang M, Jiang T, Tian L, Liu Y, Liu Z, et al. Functional dysconnectivity of the dorsolateral prefrontal cortex in first-episode schizophrenia using resting-state fMRI. *Neurosci Lett.* 2007; 417:297–302. [PubMed: 17399900]
16. Nygard M, Eichele T, Loberg EM, Jorgensen HA, Johnsen E, Kroken RA, et al. Patients with Schizophrenia Fail to Up-Regulate Task-Positive and Down-Regulate Task-Negative Brain Networks: An fMRI Study Using an ICA Analysis Approach. *Front Hum Neurosci.* 2012; 6:149. [PubMed: 22666197]
17. Metzak PD, Riley JD, Wang L, Whitman JC, Ngan ET, Woodward TS. Decreased efficiency of task-positive and task-negative networks during working memory in schizophrenia. *Schizophr Bull.* 2012; 38:803–813. [PubMed: 21224491]
18. Schlosser R, Gesierich T, Kaufmann B, Vucurevic G, Hunsche S, Gawehn J, et al. Altered effective connectivity during working memory performance in schizophrenia: a study with fMRI and structural equation modeling. *Neuroimage.* 2003; 19:751–763. [PubMed: 12880804]
19. Roebroeck A, Formisano E, Goebel R. Mapping directed influence over the brain using Granger causality and fMRI. *Neuroimage.* 2005; 25:230–242. [PubMed: 15734358]
20. Uddin LQ, Supekar KS, Ryali S, Menon V. Dynamic reconfiguration of structural and functional connectivity across core neurocognitive brain networks with development. *J Neurosci.* 2011; 31:18578–18589. [PubMed: 22171056]

21. Supekar K, Menon V. Developmental maturation of dynamic causal control signals in higher-order cognition: a neurocognitive network model. *PLoS Comput Biol.* 2012; 8:e1002374. [PubMed: 22319436]
22. Craig AD. How do you feel--now? The anterior insula and human awareness. *Nat Rev Neurosci.* 2009; 10:59–70. [PubMed: 19096369]
23. Critchley HD, Elliott R, Mathias CJ, Dolan RJ. Neural activity relating to generation and representation of galvanic skin conductance responses: a functional magnetic resonance imaging study. *J Neurosci.* 2000; 20:3033–3040. [PubMed: 10751455]
24. Spence S, Shapiro D, Zaidel E. The role of the right hemisphere in the physiological and cognitive components of emotional processing. *Psychophysiology.* 1996; 33:112–122. [PubMed: 8851239]
25. Dosenbach NU, Visscher KM, Palmer ED, Miezin FM, Wenger KK, Kang HC, et al. A core system for the implementation of task sets. *Neuron.* 2006; 50:799–812. [PubMed: 16731517]
26. Nelson SM, Dosenbach NU, Cohen AL, Wheeler ME, Schlaggar BL, Petersen SE. Role of the anterior insula in task-level control and focal attention. *Brain Struct Funct.* 2010; 214:669–680. [PubMed: 20512372]
27. Carter CS, MacDonald AW 3rd, Ross LL, Stenger VA. Anterior cingulate cortex activity and impaired self-monitoring of performance in patients with schizophrenia: an event-related fMRI study. *Am J Psychiatry.* 2001; 158:1423–1428. [PubMed: 11532726]
28. Liu SK, Chiu CH, Chang CJ, Hwang TJ, Hwu HG, Chen WJ. Deficits in sustained attention in schizophrenia and affective disorders: stable versus state-dependent markers. *Am J Psychiatry.* 2002; 159:975–982. [PubMed: 12042186]
29. Wylie KP, Tregellas JR. The role of the insula in schizophrenia. *Schizophr Res.* 2010; 123:93–104. [PubMed: 20832997]
30. Ellison-Wright I, Glahn DC, Laird AR, Thelen SM, Bullmore E. The anatomy of first-episode and chronic schizophrenia: an anatomical likelihood estimation meta-analysis. *Am J Psychiatry.* 2008; 165:1015–1023. [PubMed: 18381902]
31. Minzenberg MJ, Laird AR, Thelen S, Carter CS, Glahn DC. Meta-analysis of 41 functional neuroimaging studies of executive function in schizophrenia. *Arch Gen Psychiatry.* 2009; 66:811–822. [PubMed: 19652121]
32. First, M.; Gibbon, M.; Spitzer, R.; JBW, W.; LS, B. Structured Clinical Interview for DSM-IV Axis I Disorders, Clinician Version (SCID-CV). American Psychiatric Press, Inc.; Washington D.C.: 1997.
33. Woods SW. Chlorpromazine equivalent doses for the newer atypical antipsychotics. *J Clin Psychiatry.* 2003; 64:663–667. [PubMed: 12823080]
34. Overall JEG, D. R. The Brief Psychiatric Rating Scale. *Psychol Rep.* 1962; 10:790–812.
35. Hong LE, Schroeder M, Ross TJ, Buchholz B, Salmeron BJ, Wonodi I, et al. Nicotine enhances but does not normalize visual sustained attention and the associated brain network in schizophrenia. *Schizophr Bull.* 2011; 37:416–425. [PubMed: 19713300]
36. Deen B, Pitskel NB, Pelphrey KA. Three systems of insular functional connectivity identified with cluster analysis. *Cereb Cortex.* 2011; 21:1498–1506. [PubMed: 21097516]
37. Touroutoglou A, Hollenbeck M, Dickerson BC, Feldman Barrett L. Dissociable large-scale networks anchored in the right anterior insula subserve affective experience and attention. *Neuroimage.* 2012; 60:1947–1958. [PubMed: 22361166]
38. Chang LJ, Yarkoni T, Khaw MW, Sanfey AG. Decoding the Role of the Insula in Human Cognition: Functional Parcellation and Large-Scale Reverse Inference. *Cereb Cortex.* 2012
39. Andrews-Hanna JR, Reidler JS, Sepulcre J, Poulin R, Buckner RL. Functional-anatomic fractionation of the brain's default network. *Neuron.* 2010; 65:550–562. [PubMed: 20188659]
40. Chen G, Glen DR, Saad ZS, Paul Hamilton J, Thomason ME, Gotlib IH, et al. Vector autoregression, structural equation modeling, and their synthesis in neuroimaging data analysis. *Comput Biol Med.* 2011; 41:1142–1155. [PubMed: 21975109]
41. Smith SM, Miller KL, Salimi-Khorshidi G, Webster M, Beckmann CF, Nichols TE, et al. Network modelling methods for FMRI. *Neuroimage.* 2011; 54:875–891. [PubMed: 20817103]

42. Friston K. Dynamic causal modeling and Granger causality Comments on: the identification of interacting networks in the brain using fMRI: model selection, causality and deconvolution. *Neuroimage*. 2011; 58:303–305. [PubMed: 19770049]
43. Roebroeck A, Formisano E, Goebel R. The identification of interacting networks in the brain using fMRI: Model selection, causality and deconvolution. *Neuroimage*. 2011; 58:296–302. [PubMed: 19786106]
44. Schippers MB, Renken R, Keysers C. The effect of intra- and inter-subject variability of hemodynamic responses on group level Granger causality analyses. *Neuroimage*. 2011; 57:22–36. [PubMed: 21316469]
45. Menon V, Uddin LQ. Saliency, switching, attention and control: a network model of insula function. *Brain Struct Funct*. 2010; 214:655–667. [PubMed: 20512370]
46. Raichle ME, Snyder AZ. A default mode of brain function: a brief history of an evolving idea. *Neuroimage*. 2007; 37:1083–1090. [PubMed: 17719799]
47. Pettersson-Yeo W, Allen P, Benetti S, McGuire P, Mechelli A. Dysconnectivity in schizophrenia: where are we now? *Neuroscience and biobehavioral reviews*. 2011; 35:1110–1124. [PubMed: 21115039]
48. Fornito A, Zalesky A, Pantelis C, Bullmore ET. Schizophrenia, neuroimaging and connectomics. *Neuroimage*. 2012; 62:2296–2314. [PubMed: 22387165]
49. Chai XJ, Whitfield-Gabrieli S, Shinn AK, Gabrieli JD, NietoCastanon A, McCarthy JM, et al. Abnormal medial prefrontal cortex resting-state connectivity in bipolar disorder and schizophrenia. *Neuropsychopharmacology*. 2011; 36:2009–2017. [PubMed: 21654735]
50. Barch DM, Csernansky JG. Abnormal parietal cortex activation during working memory in schizophrenia: verbal phonological coding disturbances versus domain-general executive dysfunction. *Am J Psychiatry*. 2007; 164:1090–1098. [PubMed: 17606661]
51. Elvevag B, Goldberg TE. Cognitive impairment in schizophrenia is the core of the disorder. *Crit Rev Neurobiol*. 2000; 14:1–21. [PubMed: 11253953]
52. Hill K, Mann L, Laws KR, Stephenson CM, Nimmo-Smith I, McKenna PJ. Hypofrontality in schizophrenia: a meta-analysis of functional imaging studies. *Acta Psychiatr Scand*. 2004; 110:243–256. [PubMed: 15352925]
53. Wesnes K, Warburton DM. Effects of smoking on rapid information processing performance. *Neuropsychobiology*. 1983; 9:223–229. [PubMed: 6646394]
54. Nuechterlein KH, Dawson ME. Information processing and attentional functioning in the developmental course of schizophrenic disorders. *Schizophr Bull*. 1984; 10:160–203. [PubMed: 6729409]
55. Seeley WW, Crawford RK, Zhou J, Miller BL, Greicius MD. Neurodegenerative diseases target large-scale human brain networks. *Neuron*. 2009; 62:42–52. [PubMed: 19376066]
56. Seeley WW. Anterior insula degeneration in frontotemporal dementia. *Brain Struct Funct*. 2010; 214:465–475. [PubMed: 20512369]
57. Di Martino A, Ross K, Uddin LQ, Sklar AB, Castellanos FX, Milham MP. Functional brain correlates of social and nonsocial processes in autism spectrum disorders: an activation likelihood estimation meta-analysis. *Biol Psychiatry*. 2009; 65:63–74. [PubMed: 18996505]
58. Uddin LQ, Menon V. The anterior insula in autism: under-connected and under-examined. *Neuroscience and biobehavioral reviews*. 2009; 33:1198–1203. [PubMed: 19538989]
59. Bannister V, Ham TE, Leech R, Kinnunen KM, Mehta MA, Greenwood RJ, et al. Salience network integrity predicts default mode network function after traumatic brain injury. *Proc Natl Acad Sci U S A*. 2012; 109:4690–4695. [PubMed: 22393019]
60. David O, Guillemain I, Sallet S, Rey S, Deransart C, Segebarth C, et al. Identifying neural drivers with functional MRI: an electrophysiological validation. *PLoS Biol*. 2008; 6:2683–2697. [PubMed: 19108604]
61. Ko AL, Darvas F, Poliakov A, Ojemann J, Sorensen LB. Quasi-periodic fluctuations in default mode network electrophysiology. *J Neurosci*. 2011; 31:11728–11732. [PubMed: 21832202]



Overlap of NC and SZ

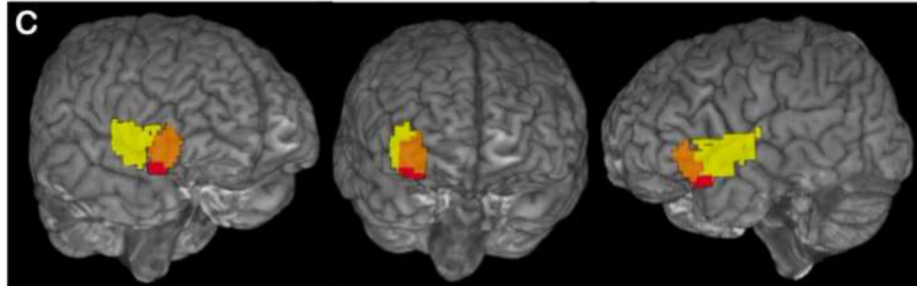


**Figure 1.** Cluster analysis of functional connectivity profiles of right insular voxel seed regions parcellated the insula into dorsal anterior (**orange**), ventral anterior (**red**) and posterior insula (**yellow**). Cluster analysis was performed separately for the two groups and demonstrates consistency of parcellation of AIns into a dorsal-ventral gradient for both (**A**) normal control (NC) and (**B**) schizophrenia (SZ) groups. Final clusters used for subsequent analyses were derived by finding the intersection of the schizophrenia and control clusters (i.e., overlapping voxels) for each insular subregion. Three-dimensional rendered views of overlap of NC and SZ clusters are depicted in (**C**) as seen from right, center and left views of brain.



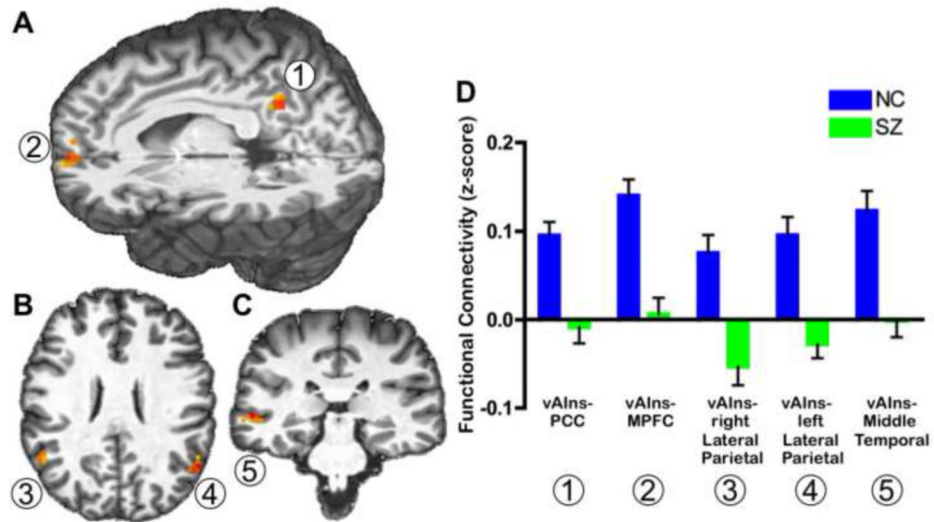


**Figure 2. Decreased connectivity between right ventral anterior insula and areas of default mode network in schizophrenia**

Areas of decreased functional connectivity ( $p_{\text{corrected}} < 0.05$ ) between right ventral AIns (vAIns) and posterior cingulate cortex (PCC) (A), medial prefrontal cortex (MPFC) (A), left middle temporal cortex (B) and bilateral lateral parietal cortex (C) in schizophrenia (SZ) compared to normal control (NC) subjects. (D) Mean  $\pm$  standard error of the mean functional connectivity (z-score) for clusters depicted in A-C.

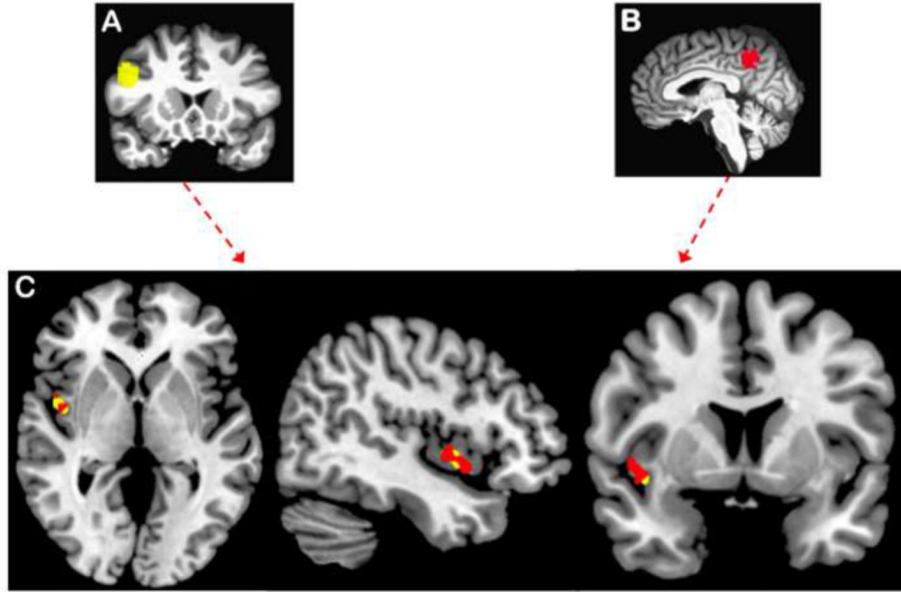


**Figure 3. Reversed functional connectivity analyses from central executive (CEN) and default mode network (DMN) seeds showed reduced connectivity exclusively with the right insula in schizophrenia**

Group differences in resting state functional connectivity analyses ( $p_{\text{corrected}} < 0.05$ ) were found using (A) a central executive network node at the right dorsolateral prefrontal cortex (**yellow**) and (B) a default mode network node at the posterior cingulate cortex (**red**) (C). Reduced connectivity between CEN/DMN and overlapping clusters in the right anterior-middle insula are depicted.

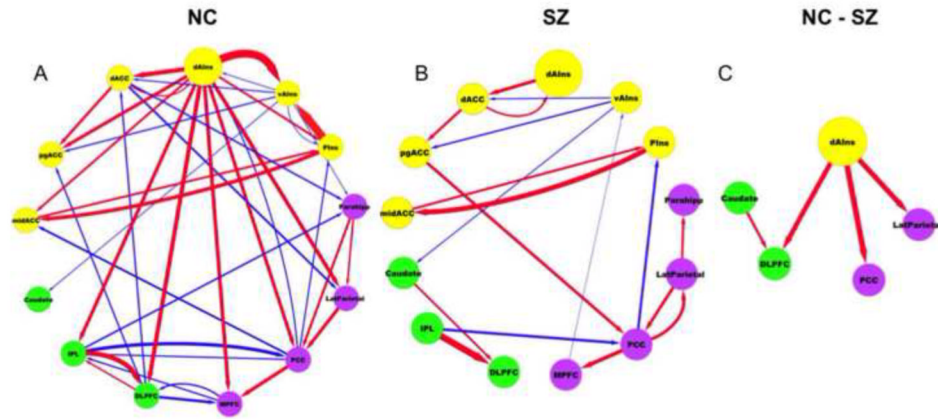


**Figure 4. Effective connectivity: Granger analysis**

(A) Normal control (NC) subjects showed significant paths from right dorsal AIns (dAIns) to areas of central executive network (CEN: **green**), salience network (SN: **yellow**), and default mode networks (DMN: **purple**). (B) In contrast, subjects with schizophrenia (SZ) had markedly reduced outflow from dAIns to CEN and DMN. (C) Group comparison reveals significantly reduced path coefficients from dAIns to areas of CEN (right dorsolateral prefrontal cortex: DLPFC) and DMN (posterior cingulate cortex: PCC, right lateral parietal cortex: LatParietal) in schizophrenia (significant after controlling for false discovery rate,  $p_{\text{corrected}} < 0.05$ ). Arrows show direction of path. Red arrows denote positive paths (activity in source predicts subsequent increases in target activity) and blue arrows denote negative paths (source predicts subsequent decreases in target). Thickness of arrows represents magnitude of path coefficients. Other abbreviations: dACC, dorsal anterior cingulate cortex; midACC, posterior part of anterior cingulate extending to middle cingulate; pgACC, pregenual anterior cingulate; vAIns, right ventral AIns; PIns, right posterior insula; IPL, right inferior parietal lobule/sulcus; MPFC, medial prefrontal cortex.

**Table 1**

Node coordinates for effective connectivity analyses

Network	ROI	Right hemisphere peak coordinates		
		x	y	z
Salience Network	Dorsal AIns (dAIns)	-	-	-
	Ventral AIns (vAIns)	-	-	-
	Posterior insula (PIIns)	-	-	-
	Dorsal anterior cingulate (dACC)	3	30	27
	Pregenuar anterior cingulate (pgACC)	3	42	12
	Dorsal/middle cingulate (midACC)	0	3	42
Central Executive Network	Dorsolateral prefrontal cortex (DLPFC)	44	45	9
	Inferior parietal lobule/sulcus (IPL)	60	-	33
	Caudate	15	15	6
Default Mode Network	Medial prefrontal cortex (MPFC)	0	60	6
	Posterior cingulate cortex (PCC)	9	-	27
	Lateral parietal cortex (LatParietal)	51	-	27
	Parahippocampal gyrus (Parahipp)	30	-	-

**Table 2**

Functional circuits with decreased connectivity in schizophrenia from seed-based functional connectivity analyses

Seed region	Area of decreased connectivity	Volume (mm <sup>3</sup> )	t	Peak activity: Talairach coordinates (LPI)		
				x	y	z
Right ventral ANs	Medial prefrontal cortex (MPFC)	1134	4.3	0	60	6
	Left lateral parietal	1026	4.8	-60	-57	24
	Right lateral parietal	486	4.1	51	-55	27
	Right middle temporal gyrus	918	4.5	60	-30	0
	Posterior cingulate cortex (PCC)	432	4.8	9	-51	27
Right dorsolateral prefrontal cortex	Right anterior-middle insula	486	4.2	40	10	0
Posterior cingulate cortex	Right anterior-middle insula	648	3.9	42	8	-9